



# Anticancer activity, DNA binding and cell mechanistic studies of estrogen-functionalised Cu(II) complexes

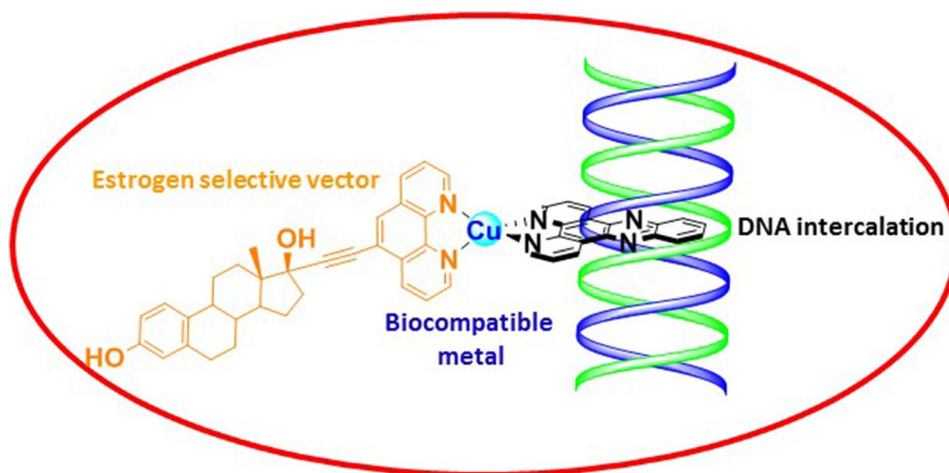
Stephen Barrett<sup>1</sup> · Michele De Franco<sup>2</sup> · Andrew Kellett<sup>3</sup> · Eithne Dempsey<sup>1</sup> · Cristina Marzano<sup>2</sup> · Andrea Erxleben<sup>4</sup> · Valentina Gandin<sup>2</sup> · Diego Montagner<sup>1</sup>

Received: 8 August 2019 / Accepted: 8 October 2019 / Published online: 26 October 2019  
© Society for Biological Inorganic Chemistry (SBIC) 2019

## Abstract

Four estrogen-functionalised copper complexes were synthesised and investigated as electrochemical active DNA binding and cleavage agents. These complexes strategically contain a biocompatible metal centre [Cu(II)], a planar aromatic ligand as DNA intercalative agent and an estradiol-derivative moiety which acts as delivery vector to target estrogen-receptor-positive (ER+) cancer cells. Cytotoxic activity was studied over a panel of estrogen-receptor-positive (ER+) and negative (ER-) human cancer cell lines by means of both 2D and 3D cell viability studies. The complexes showed high in vitro intercalative interaction with nuclear DNA and demonstrated to be strong DNA cleaving agents. This series of Cu compounds are potent anticancer agents with low and sub-micromolar IC<sub>50</sub> values and the cellular uptake follows the lipophilicity order meaning that the internalisation mainly happened via passive diffusion. Finally, the estrogen-complexes are involved in the cellular redox stress by stimulating the production of ROS (reactive oxygen species).

## Graphic abstract



**Keywords** Copper · Anticancer drug · DNA intercalation · ROS production · Estrogen · Selective target

**Electronic supplementary material** The online version of this article (<https://doi.org/10.1007/s00775-019-01732-8>) contains supplementary material, which is available to authorized users.

✉ Valentina Gandin  
valentina.gandin@unipd.it

✉ Diego Montagner  
diego.montagner@mu.ie

Extended author information available on the last page of the article

## Introduction

Copper complexes are becoming interesting developmental anticancer agents and many recent examples demonstrated the efficacy of tumour treatment with Cu-containing drugs [1, 2]. Copper complexes are considered as an alternative

to the classical platinum containing anticancer drugs (i.e., cisplatin, carboplatin, oxaliplatin) because copper, being an endogenous essential metal for most aerobic organisms, is better tolerated compared to exogenous metals. In addition, the altered copper metabolism displayed by many cancer cells as well as the differential response between normal and tumour cells to copper, laid down the rationale for the development of copper complexes as anticancer agents. Casiopeinas is the generic name of a group of copper complexes designed to be used as antineoplastics and have recently shown promising results as chemotherapeutic agents in animal models and clinical trials [3, 4]. Copper is involved in fundamental biological processes such as respiration, detoxification of ROS (reactive oxygen species) and copper-based drugs show a wide spectrum of action [5–12]. Copper is a biological redox active metal centre ( $\text{Cu}^{2+} + 1\text{e}^- \rightarrow \text{Cu}^+$   $E_0 = 0.153$  V) and it is involved in the regulation of ROS ( $\text{OH}^\cdot$ ,  $\text{O}_2^{\cdot-}$ ...) via Fenton and Haber–Weiss type reactions that are responsible for the cleavage of the DNA back-bonds [13–20]. Copper plays a major role in cancer cell oxidative stress that can result in detrimental cellular damage including lipid peroxidation, DNA damage, protein oxidation and enzyme inactivation, which in turn can lead to cell death. One of the pioneer examples of anticancer Cu(II) complexes is  $[\text{Cu}(\text{phen})_2]^{2+}$  (phen = 1,10-phenanthroline) reported by Sigman and co-workers, that showed a strong anticancer and nuclease activity in the presence of reducing agents [21, 22]. This compound also showed a strong interaction with DNA and it was able to intercalate between the DNA nucleobases due to the presence of the planar aromatic phenanthroline ligand.  $[\text{Cu}(\text{phen})_2]^{2+}$  opened the route to the synthesis of several metal complexes with DNA intercalative properties using modified phenanthroline ligands such as DPQ, DPPZ and DPPN (DPQ = dipyrido[3,2-*f*:2',3'-*h*

quinoxaline, DPPZ = dipyrido[3,2-*a*:2',3'-*c*]phenazine, and DPPN = benzo[*i*]dipyrido[3,2-*a*:2',3'-*c*]phenazine) [23–30]. These complexes showed great DNA binding affinity and anticancer properties but negligible selectivity for tumour tissues. One of the most desired properties for an anticancer drug is the selectivity for cancer cells and, furthermore, for some specific cancer tissues. Steroids are important delivery vectors that can be used for the selective targeting of the drugs toward the cancer cell [31]. The activity of estrogens, the primary female sex hormone, is mediated by the presence of estrogen receptors (ERs) in cells and ERs are over-expressed in breast, ovarian, colon and prostate cancers, which are termed ER+ [32, 33]. ERs therefore, represent interesting anticancer targets [34, 35]. Several cancers are estrogen-dependent (i.e., ovarian cancer) and estrogen derivatives are also used in the treatment of particular cancers. In turn, a host of strategies have been employed to date where derivatives of one of the three major endogenous estrogens (estrone, estradiol, and estriol) have been chemically linked to a platinum-containing anticancer drug [36–38] and radiopharmaceuticals [39]. Recently, we reported the antimicrobial and anticancer activity of steroid derivatives of Cu(II), Pt(II), and Au(I) complexes containing both the female (estradiol) and male (testosterone) steroids [40–42]. Here, we present the syntheses, chemical and electrochemical investigation, the DNA binding and cleavage properties together with a detailed biological study of the anticancer activity on 2D and 3D cancer cell cultures of a series of estrogen-functionalized Cu(II) complexes with the general formula  $[\text{Cu}(\text{N}\cup\text{N})(\text{estradiol-phen})](\text{NO}_3)_2$ , where (N $\cup$ N) is phenanthroline, DPQ, DPPZ and DPPN (Fig. 1). Some of these complexes, which display the simultaneous presence of both the non-toxic metal centre [copper(II)] and of a planar ligand for DNA intercalation properties

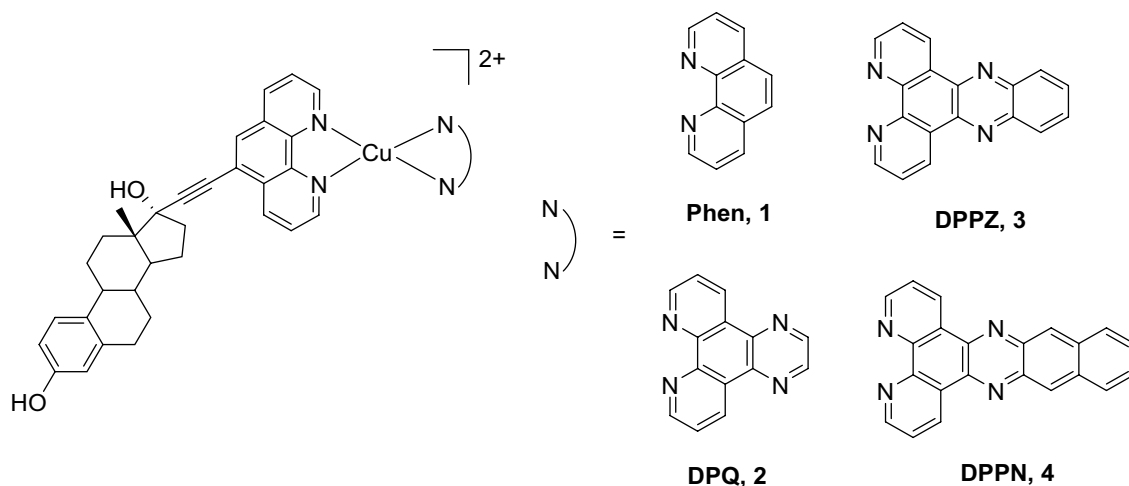


**Fig. 1** Structures of the estrogen-derivatives Cu(II) complexes

(Phen, DPQ, DPPZ and DPPN), along with the presence of an estrogen-derivative as a delivery vector to target cancer cells, showed important in vitro and in vivo antimicrobial activity against *Staphylococcus aureus* [41]. The biological activity is assessed using cancer cell lines expressing estrogen receptors (ER+) and not expressing estrogen receptors (ER-) with the aim of verifying the successfulness of copper functionalization.

## Materials and methods

All reagents and reactants were purchased from commercial sources. The two sources used were Sigma-Aldrich and Tokyo Chemical Industry. All solvents were used without further purification. The THF (Tetrahydrofuran) used for the Sonogashira coupling reaction, was dried using four angstrom molecular sieves, it was then decanted into a round bottom flask and kept under high vacuum using a Schlenk line while immersed in liquid nitrogen. The THF was then flushed with nitrogen gas. This step was repeated a minimum of three times for the Sonogashira coupling reaction. All NMR spectra were recorded on a Bruker Advance spectrometer with the probe at 293 K, operating at 500 MHz for the  $^1\text{H}$  and at 125 MHz for  $^{13}\text{C}\{^1\text{H}\}$  nuclei. Spectra were recorded in  $\text{CDCl}_3$  using  $\text{Me}_4\text{Si}$  as the internal standard. All chemical shifts are in ppm. Infrared (IR) spectra were recorded in the region  $4000\text{--}400\text{ cm}^{-1}$  on a Perkin Elmer precisely spectrum 100 FT/IR spectrometer. The solid samples were run using ATR. Elemental analyses (carbon, hydrogen and nitrogen) were performed with a PerkinElmer 2400 series II analyzer. ESI mass spectra were recorded in positive mode with a Waters LCT Premier XE Spectrometer.

**Electrochemistry:** Non-aqueous electrochemical analysis of 1 mM of the copper complexes **1–3** was carried out at a glassy carbon electrode ( $0.07\text{ cm}^2$ ) in a three electrode configuration with Pt wire counter and non-aqueous reference  $\text{Ag}/\text{Ag}^+$  reference electrode in 0.1 M  $\text{LiClO}_4/\text{DMF}$  (dimethylformamide). Glassy carbon electrodes were prepared by polishing with alumina suspension on a microcloth followed by sonication in deionised water. Voltammograms were generated over the range +1 to -1 or -2 V vs.  $\text{Ag}/\text{Ag}^+$  in a deaerated solution ( $\text{N}_2$  bubbling 10 min). Data analysis employed the third cycle of the voltammogram with cathodic scan direction at  $100\text{ mV s}^{-1}$  in all cases.

**Stability:** Compound **4** was taken as reference being the most active. **4** was dissolved in DMF to obtain a 5 mM solution. 200  $\mu\text{L}$  of this solution was diluted to 2.0 mL with phosphate buffer solution ( $\text{pH}=7.4$ ,  $[\text{P}]=50\text{ mM}$ ). The solution was kept at  $37\text{ }^\circ\text{C}$  and monitored by HPLC using a Phenomenex Luna C18 (5  $\mu\text{M}$ , 100  $\text{\AA}$ , 250 mm  $\times$  4.60 mm i.d.) column at a flow rate of 1.0 mL/min with 280 nm UV detection at room temperature. The mobile phase was 80:20

acetonitrile (0.1% trifluoroacetic acid): water (0.1% trifluoroacetic acid).

## DNA binding experiments

### Competitive ethidium displacement

A working solution of 20.0  $\mu\text{M}$  UltraPure calf-thymus DNA [CT-DNA, Invitrogen 15633-019,  $\epsilon_{260}=12,824\text{ M (bp)}^{-1}\text{ cm}^{-1}$ ] along with 25.2  $\mu\text{M}$  ethidium bromide (EtBr) in HEPES buffer (80 mM,  $\text{pH}=7.2$ ) and NaCl (40 mM) was prepared. Stock solutions of metal complexes, metal salts, and groove binding drugs were prepared at  $\sim 4.0\text{ mM}$  in DMSO (dimethylsulfoxide) and diluted further with ultra-pure water. 50  $\mu\text{L}$  of DNA-Et working solution was placed in each well of a 96-well microplate with the exception of the blanks which contained 100  $\mu\text{L}$  HEPES buffer. Serial aliquots of the tested compound were added to the working solutions and the volume was adjusted to 100  $\mu\text{L}$  in each well such that the final concentration of CT-DNA and EtBr was 10.0  $\mu\text{M}$  and 12.6  $\mu\text{M}$ , respectively. The plate was allowed to incubate at room temperature for 1 h before being analyzed using a Bio-Tek synergy HT multi-mode microplate reader with excitation and emission wavelengths being set to 530 and 590 nm, respectively. Concentrations of the tested compounds were optimized such that fluorescence was 30–40% of the initial control (i.e., 50  $\mu\text{L}$  working solution + 50  $\mu\text{L}$  HEPES buffer) at their highest reading. Each drug concentration was measured in triplicate, on at least two separate occasions, and the apparent binding constants were calculated using  $K_{\text{app}}=K_e \times 12.6/\text{C50}$  where  $K_e=9.5 \times 10^6\text{ M (bp)}^{-1}$ .

### DNA-ethidium fluorescence quenching

A working solution of 50.0  $\mu\text{M}$  UltraPure calf-thymus DNA [CT-DNA, Invitrogen 15633 019,  $\epsilon_{260}=12,824\text{ M (bp)}^{-1}\text{ cm}^{-1}$ ] along with either 10.0  $\mu\text{M}$  ethidium bromide (EtBr) or Hoechst 33258 (Sigma) in HEPES buffer (80 mM,  $\text{pH}=7.2$ ) and NaCl (40 mM) was prepared. Stock solutions of metal complexes, metal salts, free ligands and groove binding drugs were prepared at  $\sim 4.0\text{ mM}$  in DMSO and diluted further with ultra-pure water. 50  $\mu\text{L}$  of DNA-Et or DNA-Hoechst working solution were placed in each well of a 96-well microplate with the exception of the blanks which contained 100  $\mu\text{L}$  HEPES buffer and 5  $\mu\text{M}$  of either Hoechst or EtBr. Serial aliquots of the tested compound were added to the working solutions and the volume was adjusted to 100  $\mu\text{L}$  in each well such that the final concentrations of CT-DNA and EtBr/Hoechst were 25.0  $\mu\text{M}$  and 5  $\mu\text{M}$ , respectively. The plate was allowed to incubate at room temperature for 5 min before being analyzed using a Bio-Tek synergy HT multi-mode microplate reader with

excitation and emission wavelengths being set to 530 and 590 nm for Et detection or 360 nm and 460 nm for Hoechst 33258 detection. Concentrations of the tested compounds were optimized such that fluorescence was 30–40% of the initial control at their highest reading. Each drug concentration was measured in triplicate, on at least two separate occasions. From a plot of fluorescence versus added drug concentration, the  $Q$  value is given by the concentration required to effect 50% removal of the initial fluorescence of bound dye.

### Viscosity experiments

Fifteen mL dsDNA (deoxyribonucleic acid sodium salt from Salmon Testes, Sigma-Aldrich, D1626-1G) solution was prepared at  $1 \times 10^{-3}$  M in 80 mM HEPES buffer for each working sample.

Stock solutions prepared in DMSO were added according to the gradual increasing [drug]/[DNA] ( $r$ ) ratios of 0.025, 0.05, 0.075, 0.1, 0.125, 0.15, 0.175 and 0.2. Viscosity values,  $\eta$ , (unit: cP) were directly obtained by running 0# spindle in working samples at 60 rpm via DV-II-programmable digital viscometer equipped with enhanced brookfield UL Adapter at room temperature. Data were presented as  $\eta/\eta_0$  versus [compound]/[DNA] ratio, in which  $\eta_0$  and  $\eta$  refers to viscosity of each DNA working sample in the absence and presence of complex.

### Nuclease activity

Reactions were carried according to the literature procedure [29]. Briefly, in a total volume of 20  $\mu$ L using 80 mL of HEPES buffer (Fisher) at pH 7.2 with 25 mM NaCl, an aliquot of the stock complex (prepared in DMSO) was mixed with 400 ng of pUC19 (Roche) and 1  $\mu$ L of 20 mM Na-L-ascorbate. Samples were incubated at 37 °C for 3 h before being quenched with 6 $\times$  loading dye (Fermentas), containing 10 mM Tris-HCl (pH 7.6), 0.03% bromophenol blue, 0.03% xylene cyanol, 60% glycerol and 60 mM EDTA, then loaded onto agarose gel 1% containing 2.0  $\mu$ L of Gel-Red<sup>TM</sup> (10000 $\times$ ). Electrophoresis was completed at 80 V for 1.5 h using a wide mini-sub cell (Bio-Rad) in 1XTAE buffer (Millipore).

### Biological studies

Copper complexes **1–4** were dissolved in the minimum DMSO amount prior to cell culture testing. A calculated amount of the stock drug DMSO solution was added to the cell culture media to reach a final maximum DMSO concentration of 0.5%, which had no effects on cell viability. Cisplatin was dissolved in 0.9% sodium chloride solution. MTT [3-(4,5-dimethylthiazol-2-yl)-2,5-diphenyltetrazolium

bromide], cisplatin and ImmunoPure *p*-nitrophenyl phosphate (APH) were obtained from Sigma Chemical Co, St. Louis, USA.

### Cell cultures

Human colon (HCT-15) and breast (MCF-7) carcinoma cell lines were obtained from American Type Culture Collection (ATCC, Rockville, MD). Human ovarian 2008 cancer cells were kindly provided by Prof. G. Marverti (Dept. of Biomedical Science of Modena University, Italy). Human ovarian A2780 cancer cells were kindly provided by Prof. M.P.Rigobello (Dept. of Biomedical Science of Padova University, Italy). Human squamous cervical A431 carcinoma cells were kindly provided by Prof. F. Zunino (Division of Experimental Oncology B, Istituto Nazionale dei Tumori, Milan, Italy). Cell lines were maintained in the logarithmic phase at 37 °C in a 5% carbon dioxide atmosphere using RPMI-1640 medium (Euroclone) containing 10% foetal calf serum (Euroclone, Milan, Italy), antibiotics (50 units mL<sup>-1</sup> penicillin and 50  $\mu$ g mL<sup>-1</sup> streptomycin), and 2 mM L-glutamine.

### Spheroid cultures

Spheroids were initiated in liquid overlay by seeding  $1.5 \times 10^3$  A2780 or HCT-15 cells/well in phenol red free RPMI-1640 medium (Sigma Chemical Co.), containing 10% FCS and supplemented with 20% methyl cellulose stock solution. A total of 150  $\mu$ L of this cell suspension was transferred to each well of a round bottom non-tissue culture treated 96-well plate (Greiner Bio-one, Kremsmünster, Austria) to allow spheroid formation within 72 h.

### Cytotoxicity assays

#### MTT assay

The growth inhibitory effect towards adherent cancer cell lines was evaluated by means of MTT assay. Briefly,  $3\text{--}8 \times 10^3$  cells/well, dependent upon the growth characteristics of the cell line, were seeded in 96-well microplates in growth medium (100  $\mu$ L). After 24 h, the medium was removed and replaced with fresh media containing the compound to be studied at the appropriate concentration. Triplicate cultures were established for each treatment. After 72 h, each well was treated with 10  $\mu$ L of a 5 mg mL<sup>-1</sup> MTT saline solution, and after additional 5 h of incubation, 100  $\mu$ L of a sodium dodecylsulfate (SDS) solution in HCl 0.01 M were added. Following an overnight incubation, cell growth inhibition was detected by measuring the absorbance of each well at 570 nm using a Bio-Rad 680 microplate reader. Mean absorbance for each drug dose was expressed

as a percentage of the absorbance of the untreated control well and plotted vs drug concentration.  $IC_{50}$  values, the drug concentrations that reduce the mean absorbance at 570 nm to 50% of those in the untreated control wells, were calculated by four parameters logistic (4-PL) model. All the values are the means  $\pm$  SD of not less than five measurements starting from three different cell cultures.

### Acid phosphatase (APH) assay

An APH-modified assay was used for determining cell viability in 3D spheroids. Briefly, the pre-seeded spheroids were treated with fresh medium containing the compound to be studied at the appropriate concentration. Triplicate cultures were established for each treatment. After 72 h, each well was treated with 100  $\mu$ L of the assay buffer (0.1 M sodium acetate, 0.1% Triton-X-100, supplemented with ImmunoPure *p*-nitrophenyl phosphate) and, following 3 h of incubation, 10  $\mu$ L of 1 M NaOH solution was added. The inhibition of the cell growth induced by the tested complexes was detected by measuring the absorbance of each well at 405 nm, using a Bio-Rad 680 microplate reader. Mean absorbance for each drug dose was expressed as a percentage of the untreated control well absorbance (T/C) and plotted vs drug concentration.  $IC_{50}$  values, the drug concentrations that reduce the mean absorbance at 405 nm 50% of those in the untreated control wells, were calculated by four parameter logistic (4-PL) model. Evaluation was based on means from at least four independent experiments.

### Cellular uptake and DNA binding

A2780 and HCT-15 cells ( $3 \times 10^6$ ) were seeded in 75  $cm^2$  flasks in growth medium (20 mL). After overnight incubation, the medium was replaced and the cells were treated with tested compounds for 24 h. Cell monolayers were washed twice with cold PBS, harvested and counted. Samples were then subjected to three freezing/thawing cycles at  $-80$  °C, and then vigorously vortexed. The samples were treated with highly pure nitric acid (Cu:  $\leq 0.5$   $\mu$ g  $kg^{-1}$ , TraceSELECT<sup>®</sup> Ultra, Sigma Chemical Co.) and transferred into a microwave Teflon vessel. Subsequently, samples were submitted to standard procedures using a speed wave MWS-3 Berghof instrument (Eningen, Germany). After cooling, each mineralized sample was analyzed for platinum using a Varian AA Duo graphite furnace atomic absorption spectrometer (Varian, Palo Alto, CA; USA) at the wavelength of 324 nm. The calibration curve was obtained using known concentrations of standard solutions purchased from Sigma Chemical Co. purchased from Sigma Chemical Co.

For DNA binding studies, DNA was extracted and purified by a commercial spin column quantification kit (Qiagen DNeasy Blood and Tissue Kit). Only highly purified

samples (A260/A230 $\cdot$ 1.8 and A280/A260 $\cdot$ 2.0) were included for analysis to avoid any artefacts. The samples were completely dried and re-dissolved in 200  $\mu$ L of Milli-Q water (18.2 M $\Omega$ ) for at least 20 min at 65 °C in a shaking thermo-mixer, mineralized and analyzed for total Cu content by GF-AAS as described above.

### Reactive oxygen species (ROS) production

The production of ROS was measured in A2780 cells ( $10^4$  per well) grown for 24 h in a 96-well plate in RPMI medium without phenol red (Sigma Chemical Co.). Cells were then washed with PBS and loaded with 10  $\mu$ M 5-(and-6)-chloromethyl-2',7'-dichlorodihydrofluorescein diacetate acetyl ester (CM-H<sub>2</sub>DCFDA) (Molecular Probes-Invitrogen, Eugene, OR) for 25 min, in the dark. Afterwards, cells were washed with PBS and incubated with tested compounds. Fluorescence increase was estimated utilizing the wavelengths of 485 nm (excitation) and 527 nm (emission) in a Fluoroskan Ascent FL (Labsystem, Finland) plate reader. Antimycin (3  $\mu$ M, Sigma Chemical Co), a potent inhibitor of Complex III in the electron transport chain, was used as positive control.

### Comet assay

About  $4 \times 10^4$  A2780 cells were seeded in 25  $cm^2$  flasks in growth medium (6 mL). After 24 h, cells were incubated for 3 h with 2.5  $\mu$ M of tested compounds. Cells were washed twice with cold PBS, harvested, centrifuged, and DNA fragmentation was measured by the alkaline comet assay. Low melting point agarose, 300  $\mu$ L (Trevigen Inc., Gaithersburg, MD, US) was heated to 37 °C and combined with  $2 \times 10^5$  cells per mL cell suspension. Each well of a 20-well CometSlide was filled with 30  $\mu$ L of the cell/agarose suspension. The slides were placed in a 4 °C refrigerator in the dark for 15 min to solidify. Slides were then immersed in 50 mL of pre-chilled lysis solution containing Trizma base, Triton-X-100, DMSO and left at 4 °C for 30 min to facilitate cell membrane and histone removal. After draining excess liquid, the slides were transferred to 50 mL of freshly prepared (same day) alkaline DNA unwinding solution, (200 mmol  $L^{-1}$  NaOH, 1 mmol  $L^{-1}$  EDTA, pH > 13) and incubated at room temperature in the dark for 20 min. After the unwinding step, electrophoresis was performed at 21 V for 30 min. Slides were then rinsed with distilled water and fixed for 5 min in 70% ethanol. Slides were dried and stained for 5 min at 4 °C with SYBR Green I (Trevigen, Inc.,) diluted 1:10 000 in 10 mmol  $L^{-1}$  Tris pH 7.5, 1 mmol  $L^{-1}$  EDTA, drained to remove excess staining solution and thoroughly dried at room temperature in the dark.

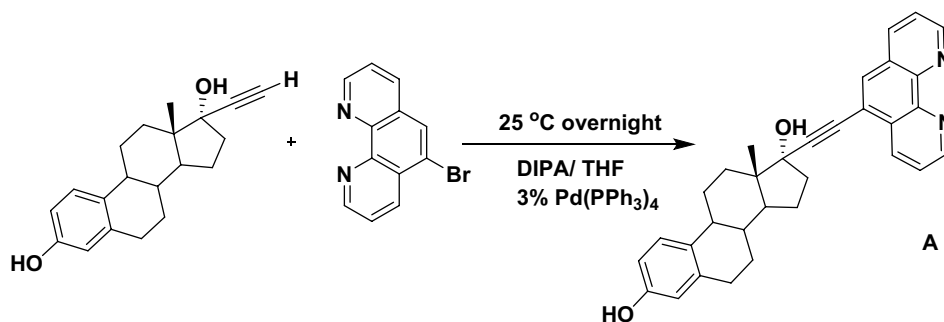
## Results and discussion

The complexes were synthesised as described in the Supporting Information (Scheme 1S). Phenanthroline-5-ethynylestradiol (**A**) is obtained using Sonogashira coupling reaction between 5-bromophenanthroline and ethynylestradiol (Scheme 1).

These kinds of reactions require extreme dry and degassed conditions and inert atmosphere; the reaction was optimized using milder conditions with respect to what was recently reported by us [41]. The yield and purity of the final product highly depend on the catalyst  $[\text{Pd}(\text{PPh}_3)_4]$  which must be freshly prepared (See Supporting Information) and stored under argon at  $-20\text{ }^\circ\text{C}$ . Briefly, **A** is synthesised by coupling 5-bromophenanthroline and ethynylestradiol in dry THF with 3% of  $[\text{Pd}(\text{PPh}_3)_4]$  as catalyst and diisopropylamine (DIPA) as a base. The replacement of  $\text{K}_2\text{CO}_3$  with the DIPA for the base and of DMF with THF for the solvent, allowed the reaction to work at r.t. with the formation of less impurities. The reaction success is evident by the disappearance of the alkyne proton resonance at 2.6 ppm in the  $^1\text{H-NMR}$  spectrum of **A** (Fig. 1S). Phenanthroline-5-ethynylestradiol (**A**), after purification, is mixed in a stoichiometric ratio 1:1 with the correspondent  $[\text{Cu}(\text{N}\cap\text{N})(\text{OH}_2)_2](\text{NO}_3)_2$  (**B–E**) (Scheme 1S), obtaining the final complexes **1–4** (Fig. 1, where  $\text{N}\cap\text{N} = \text{phen}$ —**1**;  $\text{N}\cap\text{N} = \text{DPQ}$ —**2**;  $\text{N}\cap\text{N} = \text{DPPZ}$ —**3** and  $\text{N}\cap\text{N} = \text{DPPN}$ —**4**), as described in detail in the SI. The complexes **1–4**, characterized with IR, EI. analyses, mass spectrometry, were stable up to 1 week in saline solution (0.9% NaCl). The electrochemical behavior of complexes **1–3** was investigated and Table 1 summarises the electrochemical data generated. All compounds exhibited a quasi-reversible wave when examined over the potential range 1 to  $-1\text{ V}$ , being ascribed to the  $\text{Cu}^{2+/1+}$  redox process (Fig. 1). No clear trend was evident with respect to  $\text{Cu}^{2+/1+}$   $E_{1/2}$  values for the series **1–3**, all of which fell within a similar interval ( $-0.29$  to  $-0.27\text{ V}$  vs.  $\text{Ag}/\text{Ag}^+$ ) that is within the biological range ( $-0.2$ – $0.4\text{ V}$ ) and they

are likely to undergo reduction ( $\text{Cu}^{2+} + 1\text{e}^- \rightarrow \text{Cu}^{1+}$ ) in physiological cell environment [43]. The relatively positive shift in all values for these complexes relative to that of the starting materials  $[\text{Cu}(\text{N}\cap\text{N})(\text{OH}_2)_2](\text{NO}_3)_2$  **B–D** with  $E_{1/2}$  values  $-0.456\text{ V}$  (phen),  $-0.363\text{ V}$  (DPQ) and  $-0.311\text{ V}$  (DPPZ), may reflect the electron donating contribution of the estradiol conjugate and geometric alterations upon reduction of the  $\text{Cu}^{2+}$  centres in **1–3** to the  $\text{Cu}^+$  forms. Thus, the processes may be influenced by steric effects of the ligands which overshadow electronic effects [44, 45]. The  $\Delta E_p$  values of the metal processes indicate a significant departure from a one electron reversible process, with the possibility of coupled chemical reactions and the geometric reorganisation which may accompany the  $\text{Cu}^{2+/1+}$  redox system. All  $I_{p(a)}/I_{p(c)}$  ratios are close to unity for the diffusion-controlled metal process. When the cathodic limit was extended to  $-2.0\text{ V}$  vs.  $\text{Ag}/\text{Ag}^+$  the metal underwent further one electron reduction  $\text{Cu}^{1+/0}$  with subsequent ligand dissociation and (in some cases) re-oxidation (stripping) of plated copper back to  $\text{Cu}^+$  upon anodic switching [45]. The quasi reversibility of the  $\text{Cu}^{2+/1+}$  metal processes (cathodic limit  $-1\text{ V}$  vs.  $\text{Ag}/\text{Ag}^+$ ) indicates little structural change prior to this point, after which it is likely that the complexes undergo decomposition. In the case of compounds **1** and **2**, a significant anodic shift in the  $E_{p(c)}$  values for the phenanthroline and DPQ ligands was evident ( $-1.99\text{ V}$  to  $-1.3\text{ V}$  and  $-1.92\text{ V}$  to  $-1.37\text{ V}$ , respectively). This may reflect a stabilisation of the LUMO state of the ligands, due in this case to the presence of the estradiol group, resulting in a more facile ligand reduction process. The electrochemical behaviour of natural and synthetic estrogens has been reported [46, 47] with ease of oxidation of the phenol group to the phenoxonium ion (a two electron process) being dependent on ring substitution and the solvent–electrolyte system. In these complexes, no estradiol anodic process is visible over the range examined, though clearly the presence of the steroid group influenced the phen, DPQ and DPPZ electrochemistry (Fig. 2; Table 1).

**Scheme 1** Sonogashira coupling reaction for the synthesis of phenanthroline-5-ethynylestradiol **A**



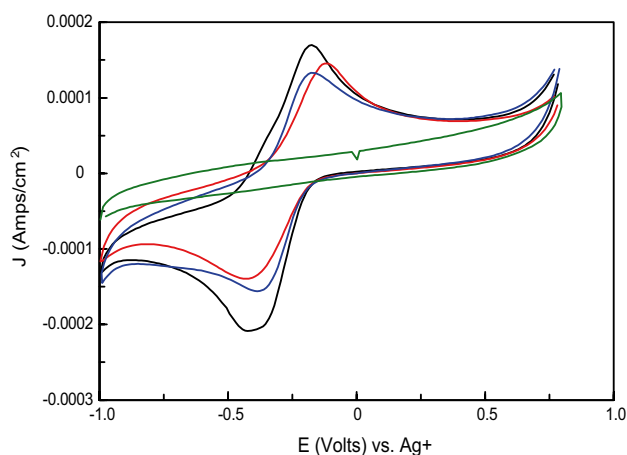


**Fig. 2** Cyclic voltammogram of 1 mM solution of complexes **1–3** at a glassy carbon electrode ( $0.07 \text{ cm}^2$ ) in a three electrode configuration with Pt wire counter and non-aqueous reference  $\text{Ag}/\text{Ag}^+$  reference electrode in 0.1 M  $\text{LiClO}_4/\text{DMF}$ . Scan rate  $100 \text{ mV s}^{-1}$  over the potential range +1 to  $-1 \text{ V}$  vs.  $\text{Ag}/\text{Ag}^+$ . Background electrolyte (green circle), (**1**) (blue circle) (**2**) (red circle) (**3**) (black circle)

### Binding affinity to calf-thymus and salmon testes DNA

The DNA binding affinity of the series of complexes was determined with calf-thymus and salmon testes duplex DNA polymers using a high throughput ethidium bromide and Hoechst 33258 fluorescence quenching assay [30], competition assay, and viscosity analyses (Fig. 3). The presence of modified phen ligands significantly enhanced the ctDNA binding affinity with  $K_{\text{app}}$  (apparent DNA binding constant) values rising from  $7 \times 10^6 \text{ M (bp)}^{-1}$  for complex **1** (phen) to  $\sim 10^7 \text{ M (bp)}^{-1}$  for complexes **2** and **3** (DPQ and DPPZ, respectively). Both phenazine complexes had a binding affinity comparable to a reference intercalating antibiotic, Actinomycin D ( $3 \times 10^7 \text{ M (bp)}^{-1}$ ) [28]. Complex **4**, containing the extended phenazine substituent DPPN, had a lower binding constant of  $\sim 5 \times 10^6 \text{ M (bp)}^{-1}$  (Table 2), an effect previously observed with copper(II) ternary complexes [29]. Fluorescence quenching ( $Q$ ) of limited Hoechst 33258 (minor groove binder) and ethidium

bromide (intercalator) bound ctDNA shows the complex series were not selective in displacing these fluorophores, however, a similar trend was observed in the displacement of both reporters:  $3 > 2 > 1 > 4$  (Table 2). Viscosity analysis with salmon testes duplex DNA confirmed complex **3**, containing the DPPZ ligand, as a strong intercalator and this hydrodynamic profile was followed by complex **2** (DPQ) and then **1** (phen, which presumably kinks DNA) [48]. Complex **4** with the larger DPPN ligand again displayed attenuated activity (Table 2). Moving from phen to DPQ and DPPZ the planarity and aromaticity of the ligands are optimized for DNA intercalation but the further modification to DPPN leads to steric hindrance thereby preventing efficient DNA binding [49, 50].

The DNA-cleavage ability of the Cu(II) complexes was measured by monitoring the conversion of SC-DNA (form I) to the nicked-circular form (NC, form II) using agarose gel electrophoresis (Fig. 4). SC pUC19 DNA (400 ng) was incubated with increasing complex concentrations (range  $0.5\text{--}20 \mu\text{M}$ ) in the presence of Na-L-ascorbate (1 mM) for 3 h. All complexes had the ability to convert SC-DNA into the nicked form at  $1 \mu\text{M}$  but complex **3**, the DPPZ-containing complex, displayed the highest cleavage potency being able to cleave plasmid DNA already at  $0.5 \mu\text{M}$  concentration. In absence of Na-L-ascorbate no detectable cleavage was observed.

With the aim of evaluating the antitumor potential of the newly developed Cu(II) complexes **1–4**, and to verify if they are more effective in targeting ER+ cell lines with respect to ER– ones, their in vitro antitumor potential was assessed in a panel of ER+ human cancer cell lines, A431 (cervical), MCF-7 (breast), 2008 (ovarian) and A2780 (ovarian) cancer cells as well as against ER- HCT-15 colon cancer cells. Cells were exposed to the tested compounds for 72 h and the  $\text{IC}_{50}$  values, calculated from the dose–response curves, are reported in Table 3. The stability of complex **4** in phosphate buffer solution ( $37 \text{ }^\circ\text{C}$ , pH 7.4) was previously evaluated via HPLC to confirm that the estrogen moiety, that can be carcinogenic being a steroid, is not released from the coordination sphere of the metal centre. Figure 3S reports the chromatograms

**Table 1** Electrochemical data for complexes **1–3**

| Complex  | Cathodic limit (V) | Cu(I/II)      |                  |                     | Cu(0/I)        |                | Ligand redox process |               |                  |  |
|----------|--------------------|---------------|------------------|---------------------|----------------|----------------|----------------------|---------------|------------------|--|
|          |                    | $E_{1/2}$ (V) | $\Delta E_p$ (V) | $I_{p(a)}/I_{p(c)}$ | $E_{p(c)}$ (V) | $E_{p(a)}$ (V) | $E_{p(c)}$ (V)       | $E_{1/2}$ (V) | $\Delta E_p$ (V) |  |
| <b>1</b> | –1                 | –0.2769       | 0.198            | 0.85                | –              | –              | –                    | –             | –                |  |
|          | –2                 | –             | –                | –                   | –              | –              | –1.3                 | –             | –                |  |
| <b>2</b> | –1                 | –0.272        | 0.296            | 1                   | –              | –              | –                    | –             | –                |  |
|          | –2                 | –             | –                | –                   | –              | –              | –1.37                | –             | –                |  |
| <b>3</b> | –1                 | –0.287        | 0.225            | 0.84                | –              | –              | –                    | –             | –                |  |
|          | –2                 | –             | –                | –                   | –1.17          | –1.365         | –1.475               | –1.42         | 0.11             |  |
|          | –2                 | –             | –                | –                   | –              | –              | –1.845               | –             | –                |  |

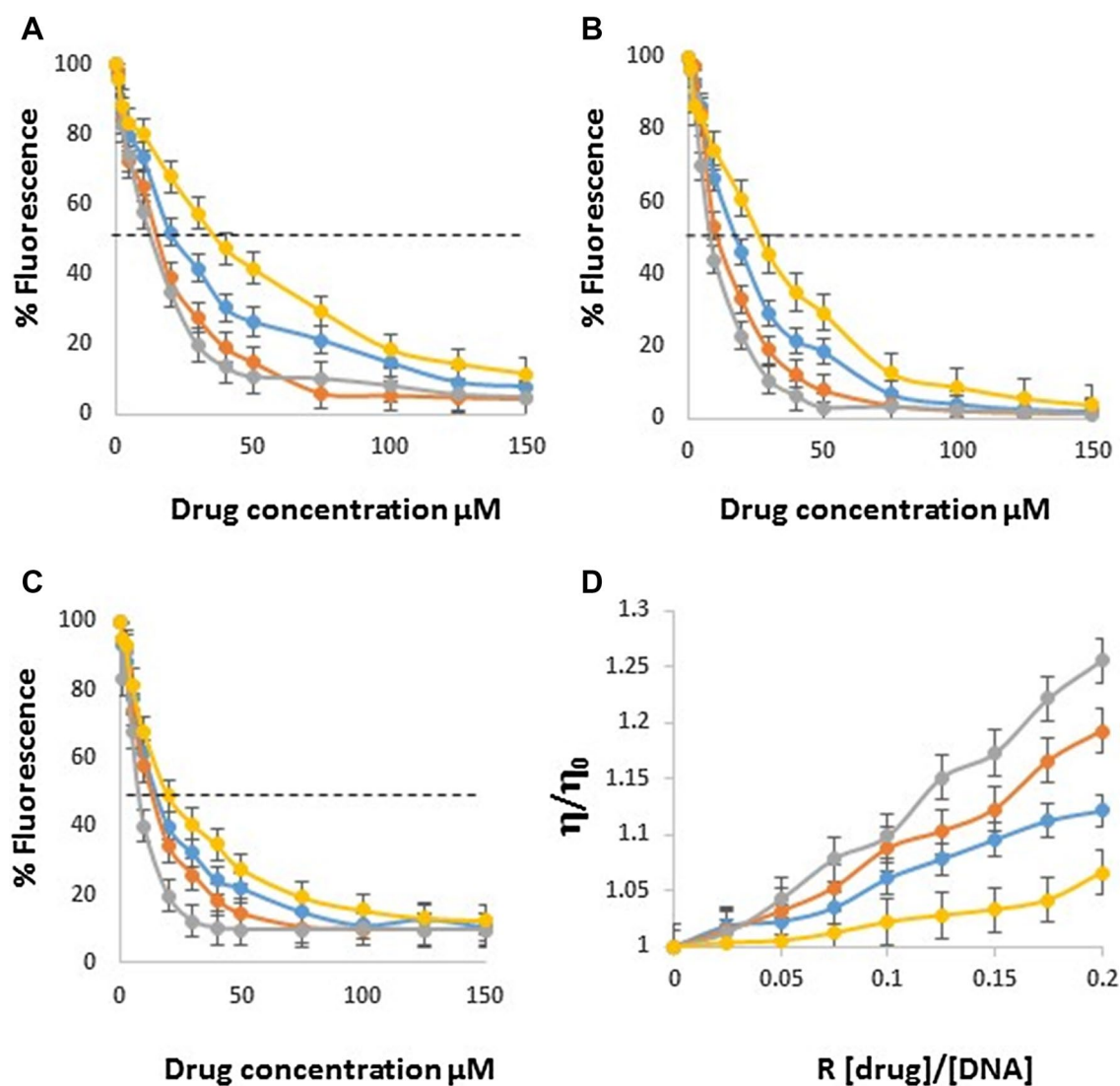


**Fig. 3** Binding of complexes **1** (blue circle), **2** (orange circle), **3** (gray circle), and **4** (yellow circle) to **A** ethidium bromide saturated solution of dsDNA (ctDNA); **B** and **C** fluorescence quenching of limited

ethidium bromide or Hoechst 33258 bound ds DNA (ctDNA) upon titration of complexes; **D** viscosity properties of complex treated salmon testes dsDNA

**Table 2** DNA binding properties of complexes 1–4

| Complex  | $C_{50}$ (μM) <sup>a</sup> | $K_{app}$ M(bp <sup>-1</sup> ) <sup>b</sup> | $Q$ (EtBr, μM) <sup>c</sup> | $Q$ (Hoechst, μM) <sup>c</sup> | $n/n_0$ ( $r=0.2$ ) <sup>d</sup> |
|----------|----------------------------|---------------------------------------------|-----------------------------|--------------------------------|----------------------------------|
| <b>1</b> | 16.13                      | $7.21 \times 10^6$                          | 21.5                        | 16.4                           | 1.12                             |
| <b>2</b> | 12.70                      | $9.43 \times 10^6$                          | 15.1                        | 12.9                           | 1.19                             |
| <b>3</b> | 8.32                       | $1.44 \times 10^7$                          | 12.5                        | 9.29                           | 1.25                             |
| <b>4</b> | 21.50                      | $5.57 \times 10^6$                          | 37.6                        | 26.1                           | 1.06                             |

<sup>a</sup> $C_{50}$  = concentration required to reduce fluorescence by 50%

<sup>b</sup> $K_{app} = K_e \times 12.6 / C_{50}$  where  $K_e = 9.5 \times 10^6$  M (bp<sup>-1</sup>)

<sup>c</sup>Reduction of 50% initial fluorescence from DNA-bound dye by tested compound (μM)

<sup>d</sup>Relative viscosity value at  $r=0.20$

**Fig. 4** DNA cleavage. Agarose gel electrophoresis patterns of SC pUC19 DNA incubated with complexes **1–4** (0.5–20  $\mu\text{M}$ ) in HEPES buffer at 37 °C for 3 h

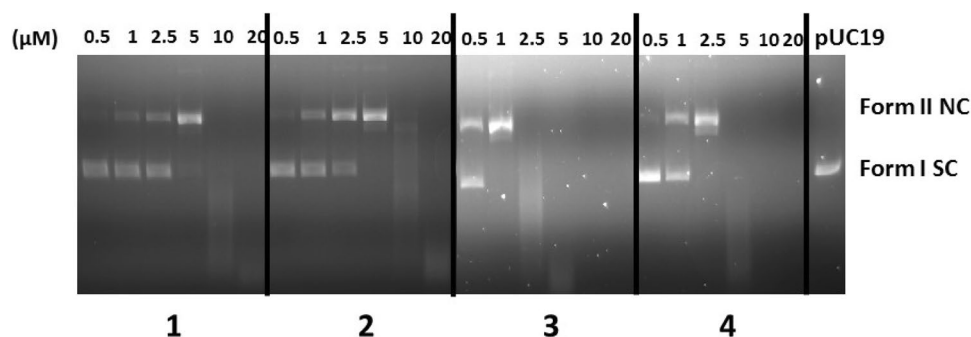


**Table 3** In vitro cytotoxic activity of complexes **1–4**

|           | IC <sub>50</sub> ( $\mu\text{M}$ ) $\pm$ SD |                |                |               |                |
|-----------|---------------------------------------------|----------------|----------------|---------------|----------------|
|           | A2780                                       | 2008           | A431           | MCF-7         | HCT-15         |
| <b>1</b>  | 0.6 $\pm$ 0.1                               | 1.5 $\pm$ 0.7  | 1.3 $\pm$ 0.3  | 1.0 $\pm$ 0.2 | 0.8 $\pm$ 0.3  |
| <b>2</b>  | 0.3 $\pm$ 0.02                              | 1.6 $\pm$ 0.4  | 2.0 $\pm$ 0.4  | 1.2 $\pm$ 0.3 | 0.8 $\pm$ 0.1  |
| <b>3</b>  | 0.1 $\pm$ 0.04                              | 0.2 $\pm$ 0.1  | 0.1 $\pm$ 0.1  | 0.7 $\pm$ 0.2 | 0.5 $\pm$ 0.2  |
| <b>4</b>  | 0.04 $\pm$ 0.01                             | 0.6 $\pm$ 0.03 | 0.3 $\pm$ 0.03 | 0.9 $\pm$ 0.2 | 0.5 $\pm$ 0.2  |
| Cisplatin | 2.6 $\pm$ 0.8                               | 2.2 $\pm$ 0.6  | 1.7 $\pm$ 0.3  | 7.6 $\pm$ 0.2 | 13.9 $\pm$ 1.7 |

Cells ( $3\text{--}8 \times 10^3 \text{ mL}^{-1}$ ) were treated for 72 h with increasing concentrations of the tested compounds. Cytotoxicity is assessed by MTT test. IC<sub>50</sub> values ( $\mu\text{M}$ ) were calculated by a four parameter logistic model ( $p < 0.05$ )

SD standard deviation

of **4** immediately upon dissolution and after 72 h where it is clearly visible that the complex is highly stable with negligible amount of steroid released.

All the complexes promoted a significant cytotoxic activity, with IC<sub>50</sub> values in the low-/sub-micromolar range against all cancer cell lines tested. In general, all derivatives were more effective in inducing cancer cell death with respect to the reference metallodrug cisplatin. Among the newly developed Cu(II) compounds, **3** and **4** were the most potent derivatives, with IC<sub>50</sub> calculated towards all tested cancer cells in the sub-micromolar range. These data indicate that by increasing the lipophilicity of the diamine ligand in turn increased the cytotoxic activity of the related copper(II) complex. On the other hand, complexes **1–3** displayed equally cytotoxic properties against ER+ and ER– cancer cells, thus suggesting the inability of these complexes to selectively target ER+ cancer cells. Conversely, **4** proved to be slightly more effective against ER+ A2780 ovarian cancer cells.

The in vitro antitumor potential of the Cu(II) complexes was also examined in 3D cell culture models of ovarian (ER+) and colon (ER–) cancers. Actually, even if the 2D cell cultures is the most used in vitro method for screening of potential therapeutics due to its simplicity, reproducibility, and low cost, this method is unable to reproduce the

**Table 4** In vitro cytotoxicity against ovarian and colon cancer cell spheroids

|           | IC <sub>50</sub> ( $\mu\text{M}$ ) $\pm$ SD |                |
|-----------|---------------------------------------------|----------------|
|           | A2780                                       | HCT15          |
| <b>1</b>  | 10.6 $\pm$ 1.0                              | 7.7 $\pm$ 1.6  |
| <b>2</b>  | 7.7 $\pm$ 1.0                               | 9.9 $\pm$ 1.0  |
| <b>3</b>  | 4.1 $\pm$ 0.1                               | 9.2 $\pm$ 0.6  |
| <b>4</b>  | 3.0 $\pm$ 0.02                              | 8.6 $\pm$ 0.5  |
| Cisplatin | 91.3 $\pm$ 5.4                              | 68.3 $\pm$ 2.1 |

Spheroids ( $1.5 \times 10^3$  cells/well) are treated for 72 h with increasing concentrations of test compounds. The growth inhibitory effect was evaluated by means of the APH test. IC<sub>50</sub> values were calculated from the dose-survival curves by the four parameter logistic model ( $p < 0.05$ )

SD standard deviation

properties of in vivo solid tumors. 3D cell cultures, possessing several features that more closely mimic the heterogeneity and complexity of in vivo tumors, are recognized to be more predictive for in vivo results than conventional 2D cell cultures [51]. The cancer spheroids were treated with copper(II) complexes or cisplatin for 72 h and cell viability was assessed by means of the acid phosphatase (APH) assay (Table 4).

These tested non-proliferative and very resistant tumour models, **1–4** were extremely effective, being more active than cisplatin against both A2780 ovarian and HCT-15 colon cancer cell spheroids. In particular, **3** and **4** were confirmed as the most potent derivatives, being about 30 and 9 times more effective than cisplatin in A2780 and HCT-15 3D cell cultures, respectively.

Complexes **1–3** showed a similar activity toward ER+ and ER– cancer cells, thus confirming the results obtained in the 2D system and supporting the hypothesis of their inability to selectively target ER+ cancer cells. On the contrary, in 3D systems, compound **4** again showed a certain degree of selectivity towards A2780 cancer cells, being about 3 times more effective in ER+ human ovarian cancer cells with respect to ER– human colon cancer cells. With the aim of identifying a possible correlation between cytotoxic

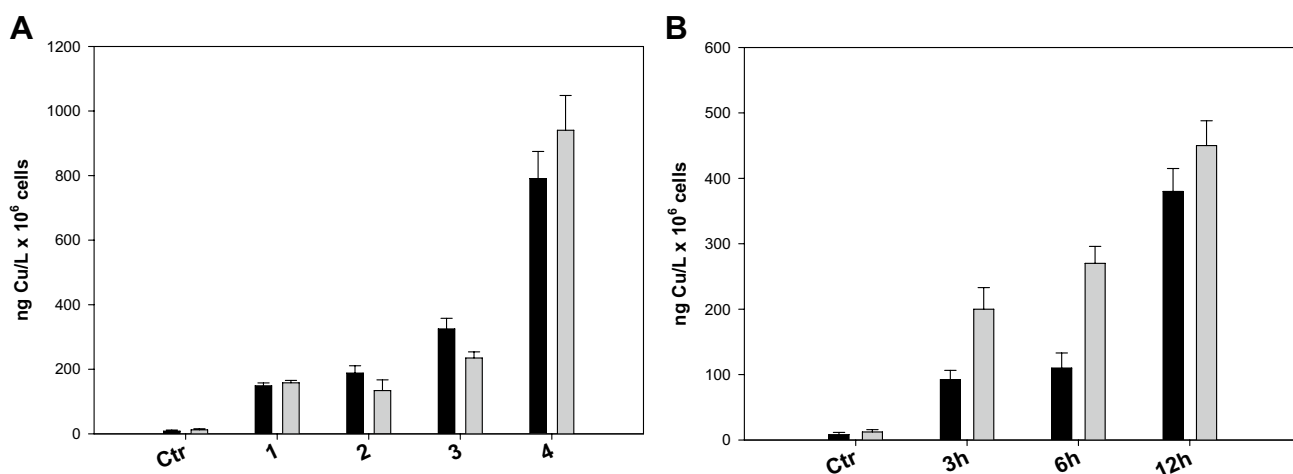


**Fig. 5** Cellular uptake in A2780 (grey bars) and HCT-15 (black bars) cancer cells. **A** Cancer cells were incubated with 0.5  $\mu\text{M}$  of copper complexes for 24 h, and cellular copper content was detected by GF-

AAS analysis. **B** Cancer cells were incubated with 0.5  $\mu\text{M}$  of copper complex **4** for 3, 6 or 12 h, and cellular copper content was detected by GF-AAS analysis. Error bars indicate the standard deviation

activity and cellular accumulation, cellular copper content was measured in ER+ A2780 and ER– HCT-15 cancer cells treated for 24 h with equimolar concentrations of the tested compounds. The cellular copper levels were quantified by means of GF-AAS analysis, and the results, expressed as ng Cu per  $10^6$  cells, are shown in Fig. 5A.

Although to a different extent, all derivatives were able to cross the cancer cell membrane and enter cancer cells. Complexes **1–3** were able to similarly accumulate into ovarian and colon cancer cells, whereas derivative **4** was significantly more effective in entering ER+ A2780 cancer cells. Interestingly, **4** accumulated in a time-dependent manner, actually both ovarian and colon cancer cells displayed a time-dependent increase in cellular copper content (Fig. 5B). By matching cytotoxic activity data with those arising from cellular uptake quantification, a linear and direct correlation is evidenced (Fig. 4S).

Copper species have been regarded as redox active compounds and it was shown that copper complexes may catalyze the reaction of hydrogen peroxide in the form of Fenton-like reactions inside the cell to produce ROS, thus altering cellular redox homeostasis and driving cells towards oxidative stress. On these bases, we evaluated cellular ROS levels in A2780 cells treated with 10  $\mu\text{M}$  of the most effective complex **4**. ROS production was monitored using the peroxide-sensitive fluorescent probe CM-H<sub>2</sub>DCFDA [5-(and-6)-chloromethyl-2',7'-dichlorodihydrofluorescein diacetate, acetyl ester]. Antimycin, a classical inhibitor of the mitochondrial respiratory chain at the level of complex III, was used as a positive control.

The results, expressed as arbitrary units of fluorescence as a function of time, are shown in Fig. 6A. Interestingly, **4** was able to substantially stimulate the production of hydrogen peroxide in a time-dependent manner, to a rather

similar extent as the respiratory chain complex III inhibitor, antimycin.

In addition, we confirmed the results obtained in cell-free experiments (DNA binding, cleavage and viscosimetry studies) and we assessed the ability of the newly synthesised copper(II) complexes to bind and to damage the DNA within intact cancer cells. The DNA damage in A2780 cells was studied after treatment with **4** for 3 h, using alkaline single cell gel electrophoresis (Comet assay, Fig. 6B). The results were compared with those obtained after treatment of A2780 cells with equitoxic concentrations of dichloro(1,10-phenanthroline)copper(II), [Cu(phen)]. Similar to [Cu(phen)], the **4**-treated cells displayed a statistically significant increase in electrophoretic migration of the DNA fragments, evidenced by well-formed comets. To analyze the cellular DNA binding, cells A2780 were treated with complexes **1–4** for 24 h, as described in the experimental section, and the amount of copper covalently bound to the extracted DNA was determined via GF-AAS. All the complexes showed very little capacity to bind to the DNA in a covalent mode comparison to the endogenous Cu control (Fig. 5S), confirming that the interaction between the complexes and DNA is purely electrostatic (intercalation).

These results confirmed the ability of these copper(II) complexes to target DNA in intact cancer cells.

## Conclusions

Four copper(II)-based complexes containing the female steroid estradiol, were synthesised with the aim to selectively target cancer cells overexpressing the estrogen receptors. The complexes proved to be very effective against all

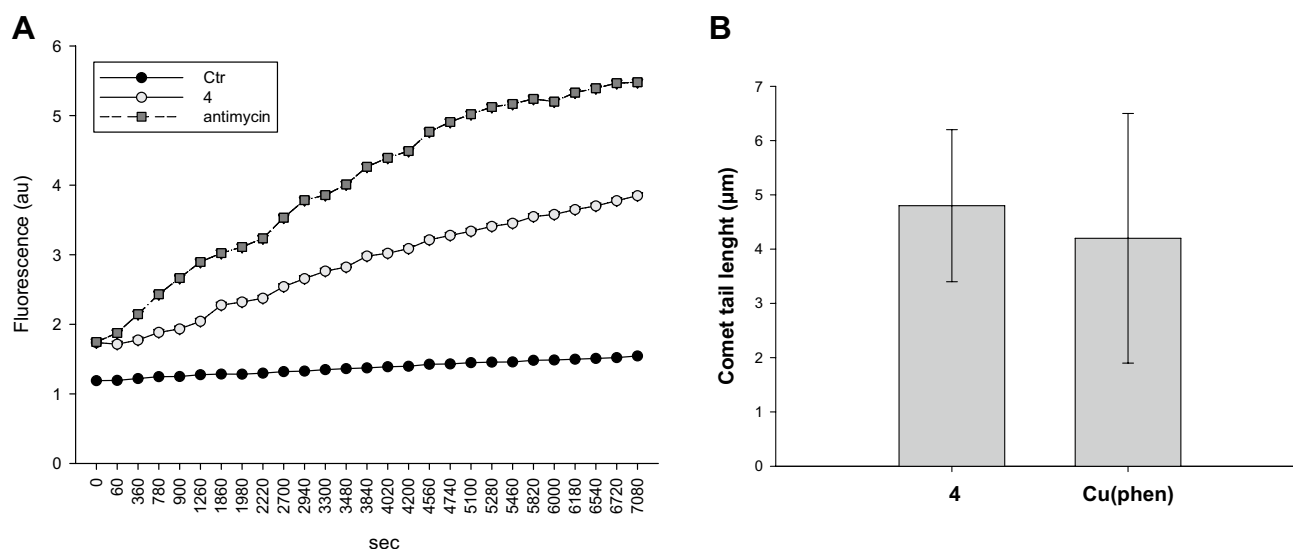


**Fig. 6** Mechanistic studies: ROS production (**a**) and DNA damage (**b**) in A2780 cancer cells. **A** Cells were preincubated in PBS/10 mM glucose medium for 20 min at 37 °C in the presence of 10 µM CM-DCFDA and then treated with derivative **4** (10 µM) or antimycin (3 µM). The fluorescence of DCF was measured as reported in the

the cancer cell lines examined (low and sub µM  $IC_{50}$  values), much more with respect to the reference drug cisplatin, complex **4** being the most effective one. Although no selectivity was observed for ER+ with respect to ER− cells for complexes **1–3**, for complex **4** a slight difference in anti-cancer potential towards ER+ cancer cells was underlined. Actually, a linear correlation was obtained in ER+ cancer cells between drug uptake and  $IC_{50}$  values. In general, the antiproliferative activity and cellular uptake increased with the lipophilic character of Cu(II) complexes, thus indicating that cellular internalisation is principally due to a passive diffusion mechanism with a minimum role of the estrogen moiety. From a mechanistic point of view, cell-free fluorescent analyses evidenced for all copper complexes strong intercalation properties but a discrimination between major and minor groove was not observed. Cu(II) complexes were redox active at the physiological range and were able to cleave DNA at very low concentrations (0.5 µM) in the presence of a reducing agent. More interestingly, cell studies confirmed their ability to target DNA and to induce ROS production in ER+ human cancer cells.

**Acknowledgements** SB is grateful to the Department of Chemistry of Maynooth University for sponsoring the postgrad scholarship. Maynooth University, Dublin City University, NUIG, University of Padova, the Italian Ministero dell'Università e della Ricerca (MIUR), and the Inter-University Consortium for Research on the Chemistry of Metal Ions in Biological Systems (CIRCMSB) are gratefully acknowledged.

experimental section. **B** A2780 cells were treated for 3 h with 0.5 µM of compound **4** and then processed for the comet assay as reported in the experimental section. Comet tail length was calculated from the center of the cell and measured in micrometers with ImageJ software. The error bars indicate the standard deviation

## Compliance with ethical standards

**Conflict of interest** There are no conflicts to declare.

## References

- Santini C, Pellei M, Gandin V, Porchia G, Tisato F, Marzano C (2014) *Chem Rev* 114:815–862
- Kellett A, Molphy Z, McKee V, Slatore C (2019) Recent advances in anticancer copper compounds. In: Casini A, Vessieres A, Meier-Menches SM (eds) Chapter 4, Metal based anticancer agents. The Royal Society of Chemistry, pp 91–119. <https://doi.org/10.1039/9781788016452-00091>
- Trejo-Solis C, Jimenez-Farfan D, Rodriguez-Enriquez S, Fernando-Valverde F, Cruz-Salgado A, Ruiz-Azuare L, Sotelo J (2012) *BMC Cancer* 12:156
- Silva-Platas C, Villegas CA, Oropeza-Almazán Y, Carrancá M, Torres-Quintanilla A, Lozano O, Valero-Elizondo J, Castillo EC, Bernal-Ramírez J, Fernández-Sada E, Vega LF, Treviño-Saldaña N, Chapoy-Villanueva H, Ruiz-Azuara L, Hernández-Brenes C, Elizondo-Montemayor L, Guerrero-Beltrán CE, Carvajal K, Bravo-Gómez ME, García-Rivas G (2018) *Oxid Med Cell Longev*. <https://doi.org/10.1155/2018/8949450> (ID 8949450)
- Ming LJ (2003) *Med Res Rev* 23:697–762
- Yu Y, Kalinowski DS, Kovacevic Z, Siafakas AR, Jansson PJ, Stefani C, Lovejoy DB, Sharpe PC, Bernhardt PV, Richardson DR (2009) *J Med Chem* 52:5271–5294
- Chen D, Peng F, Cui QC, Daniel KG, Orlu S, Liu J, Dou QP (2005) *Front Biosci* 10:2932–2939
- Chen ZF, Tan MX, Liu LM, Liu YC, Wang HS, Yang B, Peng Y, Liu HG, Liang H, Orvig C (2009) *Dalton Trans* 48:10824–10833

9. Laws K, Binjeva-Todd G, Eskandari A, Lu C, O'Reilly N, Suntharalingam K (2018) *Angew Chem Int Ed* 57:287–291
10. Lu C, Laws K, Eskandari A, Suntharalingam K (2017) *Dalton Trans* 46:12785–12789
11. Balzarini J, Keyaerts E, Vijgen L, Vandermeer F, Stevens M, De Clercq E, Egberink H, Van Ranst M (2006) *J Antimicrob Chemother* 57:472–481
12. Kellett A, Molphy Z, Slator C, McKee V, Farrell NP (2019) *Chem Soc Rev* 48:971–988
13. Molphy Z, Montagner D, Bhat SS, Slator C, Long C, Erxleben A, Kellett A (2018) *Nucleic Acid Res* 46:9918–9931
14. Fleming AM, Muller JG, Li L, Burrows CJ (2011) *Org Biomol Chem* 9:3338–3348
15. Buchtik R, Travnicek Z, Vanco J (2012) *J Inorg Biochem* 116:163–171
16. Montagner D, Gandin V, Marzano C, Erxleben A (2015) *Inorg Chim Acta* 445:101–107
17. Jopp M, Becker J, Becker S, Miska A, Gandin V, Marzano C, Schindler S (2017) *Eur J Med Chem* 132:274–281
18. Slator C, Molphy Z, McKee V, Long C, Brown T, Kellett A (2018) *Nucleic Acid Res* 46:2733–2750
19. Müller S, Versini A, Sindikubwabo F, Belthier G, Niyomchon S, Pannequin J, Grimaud L, Cañeque T, Rodriguez R (2018) *PLoS One* 13:e0208213
20. Zuin Fantoni N, Molphy Z, Slator C, Menounou G, Toniolo G, Mitrikan G, McKee V, Chatgililoglu C, Kellett A (2019) *Chem Eur J* 25:221–237
21. Sigman DS, Zelenko O, Gallagher J, Xu Y (1998) *Inorg Chem* 37:2198–2204
22. Meijler MM, Zelenko O, Sigman DS (1997) *J Am Chem Soc* 119:1135–1136
23. Zhou H, Zheng C, Zou G, Tao J (2002) *Gong D. Int J Biochem Cell Biol* 34:678–684
24. Pitie M, Donnadiou B, Meunier B (1998) *Inorg Chem* 37:3486–3489
25. Trejo-Solis C, Jimenez-Farfan D, Rodriguez-Enriquez S, Fernandez-Valverde F, Cruz-Salgado A, Ruiz-Azuara R, Sotelo J (2012) *BMC Cancer* 12:1471–2407
26. Thomas AM, Nethaji M, Mahadevan S, Chakravarty AR (2003) *J Inorg Biochem* 94:171–178
27. Charefa F, Sebtia N, Arrara L, Djarmounia M, Boussoulima N, Baghiana A, Khennouf S, Damend SAL, Mubarakd MS, Peterse DG (2015) *Polyhedron* 85:450–456
28. Tummalapalli K, Vasavi CS, Munusami P, Pathak M, Balamurali MM (2017) *Int J Biol Macromol* 95:1254–1266
29. Molphy Z, Prisecaru A, Sleitor C, Barron N, McCann M, Collieran J, Chandran D, Gathergood N, Kellett A (2014) *Inorg Chem* 53:5392–5404
30. McCann M, McGinley J, Ni K, O'Connor M, Kavanagh K, McKee V, Collieran J, Deveraux M, Gathergood N, Barron N, Prisecaru A, Kellett A (2013) *Chem Commun* 49:2431–2433
31. Le Bideau F, Dagorne S (2013) *Chem Rev* 113:1193–7850
32. Provencher-Mandeville J, Descoteaux C, Mandal SK, Leblanc V, Asselin E, Berube G (2008) *Bioorg Med Chem Lett* 18:2282–2287
33. Provencher-Mandeville J, Debnath C, Mandal SK, Leblanc V, Parent S, Asselin E, Berube G (2011) *Steroids* 76:94–103
34. Sanchez-Cano C, Huxley M, Ducani C, Hamad AE, Browning M, Navarro-Ranninger C, Quiroga AG, Rodger A, Hannon MJ (2010) *Dalton Trans* 39:11365–11374
35. Huxley M, Sanchez-Cano C, Browning MJ, Navarro-Ranninger C, Quiroga AG, Rodger A, Hannon MJ (2010) *Dalton Trans* 39:11353–11364
36. Altman J, Castrillo T, Beck W, Bernhardt G, Schoenenberger H (1991) *Inorg Chem* 30:4085–4088
37. Kenny RG, Marmion CJ (2019) *Chem Rev* 119:1058–1137
38. Saha P, Descôteaux C, Brasseur K, Fortin S, Leblanc V, Parent S, Asselin E, Bérubé G (2012) *Eur J Med Chem* 48:385–390
39. Linden HM, Peterson LM, Fowler AM (2018) *PET Clin* 13:415–422
40. Velle A, Maguire R, Kavanagh K, Montagner D, Sanz-Miguel PJ (2017) *ChemMedChem* 12:841–844
41. Barrett S, Delaney S, Kavanagh K, Montagner D (2018) *Inorg Chim Acta* 479:261–265
42. Kitteringham E, Andriollo E, Gandin V, Montagner D, Griffith D (2019) *Inorg Chim Acta* 495:118944. <https://doi.org/10.1016/j.ica.2019.05.043>
43. Zheng P, Eskandari A, Lu C, Laws K, Aldous L, Suntharalingam K (2019) *Dalton Trans* 48:5892–5896
44. Magni M, Colomba A, Dragonetti C, Mussini P (2014) *Electrochim Acta* 141:324–330
45. Justin Thomas KR, Tharmaraj P, Chandrasekhar V, Bryan D, Cordes AW (1994) *Inorg Chem* 33:5382–5390
46. Mitrofanov M, Manowong M, Roussel Y, Brandes S, Guillard R, Bessmertbykh-Lemeune A, Chen P, Kadish KM, Goulioukina N, Beletskaya I (2014) *Eur J Inorg Chem* 2014:3370–3386
47. Ngundi MN, Sadik OA, Yamaguchi T, Suye SI (2003) *Electrochim Commun* 5:61–67
48. Niyazi H, Hall JP, O'Sullivan K, Winter G, Sorensen T, Kelly JM, Cardin CJ (2012) *Nat Chem* 4:621–628
49. McGivern TJP, Slator C, Kellett A, Marmion CJ (2018) *Mol Pharm* 15:5058–5071
50. Ude Z, Kavanagh K, Twamley B, Pour M, Gathergood N, Kellett A, Marmion CJ (2019) *Dalton Trans* 48:8578–8593
51. Kunz-Schughart LA, Freyer JP, Hofstaedter F, Ebner R (2004) *J Biomol Screen* 9:273–282

**Publisher's Note** Springer Nature remains neutral with regard to jurisdictional claims in published maps and institutional affiliations.

## Affiliations

Stephen Barrett<sup>1</sup> · Michele De Franco<sup>2</sup> · Andrew Kellett<sup>3</sup> · Eithne Dempsey<sup>1</sup> · Cristina Marzano<sup>2</sup> · Andrea Erxleben<sup>4</sup> · Valentina Gandin<sup>2</sup> · Diego Montagner<sup>1</sup> 

<sup>1</sup> Department of Chemistry, Maynooth University, Maynooth, Ireland

<sup>2</sup> Department of Pharmaceutical and Pharmacological Sciences, University of Padova, Padua, Italy

<sup>3</sup> School of Chemical Sciences and National Institute for Cellular Biotechnology, Dublin City University, Glasnevin, Dublin 9, Ireland

<sup>4</sup> School of Chemistry, National University of Ireland Galway, Galway, Ireland